ILASS Americas 27th Annual Conference on Liquid Atomization and Spray Systems, Raleigh, NC, May 2015

Spray Analysis of an Electrostatic Atomization Nozzle with High Viscosity Vegetable Oils

P.W. Vesely[1,3]*, J.S. Shrimpton[1,2], F. Mashayek[1], R.J. Schick[3], and M. Thenin[3]

[1]Department of Mechanical and Industrial Engineering
University of Illinois at Chicago
Chicago, IL 60607, USA

[2]Faculty of Engineering and the Environment
University of Southampton
Highfield, Southampton, S017 1BJ, UK

[3]Spraying Systems Co.
P.O. Box 7900
Wheaton, IL 60187, USA

Abstract

Oil coating applications can be found in various industries; such as the baking industry for pan coating and in manufacturing for stamping operations. Spraying oil by the traditional means of hydraulic and air atomization presents many issues, primarily, the mess and wasted material due to overspray and the high energy cost associated with heating and spraying with compressed air. In this study, soybean oil was sprayed via a charge injection, electrostatic atomization nozzle. The oil was sprayed at room temperature with enough pressure to produce the desired flowrates through the small orifice diameters tested. The primary focus of this study was to characterize the spray plume generated from the nozzle by experimental results acquired with an Artium phase Doppler interferometer (PDI), LaVision laser sheet imaging (LSI) and an Olympus i-Speed TR camera. These systems were used to measure the spray shape, size and distribution as well as droplet size and velocity. It was found that the electrostatic atomization nozzle produced a full cone spray pattern with a Sauter mean diameter of the droplets ranging from approximately 120 to 160 microns in the main spray plume and around 30 to 40 microns outside the spray plume.

*Corresponding Author: Paul.Vesely@spray.com

Introduction

Oil coating applications can be found in many industries, from steel and material processing, manufacturing, to the food processing industry. In the material processing and manufacturing industries, oil coatings are used for lubrication, corrosion inhibition, and cooling. In the food processing industry, oil coatings are typically used to apply ingredients and as release agents. In all of these uses, the goal is to apply an even coating of oil of known weight per unit area with minimal overspray. Overspray is the oil that does not collect and stay on the target being coated. Overspray results in wasted oil, the undesired collection of oil on surrounding surfaces and the need to filter oil from the surrounding air to reduce the risk of developing a combustive environment and to maintain air quality standards.

Traditionally, oil is sprayed using hydraulic nozzles; high pressure is used to generate the kinetic energy necessary to overcome the viscosity and surface energy density to generate atomization. The kinetic energy of the oil exiting the nozzle shears the oil jet into a spray plume of various droplet sizes and velocities. Larger droplets generally hit the intended target to be coated but may ricochet off, resulting in overspray. Smaller droplets with low velocities may get carried off by the air currents generated by the nozzle spray. These smaller droplets result in the majority of the overspray. Droplet sizes of 10 microns and under can penetrate deep into a person's lungs and pose significant health risks resulting in the need for filtration [1].

In many cases, oil is heated before it is sprayed to reduce its viscosity to obtain a more uniform spray pattern. Heating also increases the amount of small droplets that do not collect on the intended target [2]. Spraying hot oil may lead to uncomfortable and dangerous work conditions by increasing the air temperature in the environment around the process and by being a burn hazard if anyone was to come in contact with it. Heating oil can add significant cost to an oil coating process as well.

Spraying oil by electrostatic atomization using a charge injection nozzle atomizes oil without the need to heat or apply high pressures while reducing overspray. The repulsive forces of the electrons injected into the oil generate the energy and motion to overcome the surface tension of the oil resulting in atomization of the fluid.

The focus of this study was to analyze the spray characteristics of an electrostatic atomization nozzle spraying pure soybean oil. This study experimentally investigated drop size, velocity and spray pattern concentration for various flow rates, orifice diameters and spray heights while the charge injection nozzle was operating near maximum spray specific charge before partial breakdown condition.

Background

Charge injection atomizers have been studied for decades and fall into two major categories; single electrode and two electrode nozzles. Single electrode nozzles consist of only a high voltage electrode. The dielectric fluid flows past the electrode as it flows through a capillary tube. The target being sprayed makes up the second (ground) electrode. The high voltage generates a Taylor cone of the fluid at the tip of the capillary tube in which a small jet of the liquid flows from the end of the cone, which then breaks up into small droplets. This process is called electrostatic spraying and has been studied extensively by Kim et al. [3] and Robinson et al. [4] among others. Electrostatic spraying works well for semiconductive fluids but provides low charge injection and requires low flow rates.

Two electrode charge injection atomizers contain both the high voltage and ground electrodes together in the nozzle. The dielectric fluid flows between the two electrodes before exiting the nozzle through an orifice. The fluid exits as a solid jet which then breaks up into individual droplets when the electrons move to the surface of the jet and overcome the surface tension forces. This process is called electrostatic atomization and has been studied extensively by Yule et al. [5], Shrimpton et al. [6], Rigit et al. [7] among others. Electrostatic atomization works for electrically insulating liquids like diesel and jet fuel as well as with vegetable oils. This type of charge injection can work with high pressures, Ergene et al. [8], and can work with larger flow rates while provide higher charge injection than electrostatic spraying nozzles. This study is on an electrostatic atomization nozzle with a single orifice operating with steady voltage and flow rate.

Experimental Setup

The oil used in this study is 100% food-grade soybean oil, the properties of which can be found in Table 1. The density of the oil was measured using a pycnometer and was found to be slightly less than that of water. The surface tension was measured using a Kruss K20 tensiometer and it was found to be about half that of water. The refractive index of the oil was measured using a Reichert AR200 Digital Refractometer. This property was utilized in the setup of the phase Doppler system used to measure droplet size and velocity in this study. Dynamic viscosity was measured using a Brookfield DV-II viscometer. A constant viscosity value was measured for various

shear rates demonstrating that the soybean oil is a Newtonian fluid. Distilled water was used as the reference material for the above mentioned devices.

Property	Value
Density, ρ (g/ml)	0.914
Dynamic Viscosity, μ (cP)	61.0
Surface Tension, σ (dyn/cm)	33.0
Refractive Index, n	1.474
Electrical Resistivity, ρ_e $(10^{10}\ \Omega m)$	23.7 [9]

Table 1. Properties of Soybean Oil

A schematic of the nozzle setup used in this study is shown in Fig. 1. A pressure pot was used to deliver oil to the nozzle. The oil was filtered with two 10 micron oil filters connected in parallel to reduce the overall pressure drop across the filters. A rotameter style flow meter with a 150 mm scale, which had a 1 mm resolution, was used to measure the volumetric flow rate of the oil. The rotameter was calibrated for the soybean oil by timing the collection of the oil in a graduated cylinder. Three collections were taken at thirteen different heights on the rotameter scale. A fourth order polynomial was fit to the data collected and was used to relate the float height for the rotameter to a volumetric flow rate for the oil. A high precision needle valve was used to control the oil flow rate and a 100 psi digital pressure gauge was used to measure the pressure at the nozzle.

The nozzle used in this study is a 3rd generation electrostatic atomizer designed by Rigit and Shrimpton [7], [10] and is shown in Fig. 2. This design features a guide for the electrode to keep it centered over the orifice and allows for the inter-electrode gap, L, to be easily adjusted. This adjustment was done using a micrometer head with a non-rotating spindle that has a resolution of 0.0254 mm (0.001 in). Removable orifice plates attach to the bottom of the nozzle allowing the flexibility to easily test various orifice diameters, d. These features are shown in the nozzle schematic shown in Fig. 3. A blunt tungsten rod with its sharp edges removed made up the high voltage electrode in this nozzle providing a plane-to-plane charge injection atomizer. This design effectively makes a capacitor with the nozzle body being the ground electrode and the oil as the dielectric medium. The charge that builds up on the electrode surface is pulled off by the moving oil and is also believed to be injected into the oil through an electrochemical process [11] resulting in strong levels of charge injection.

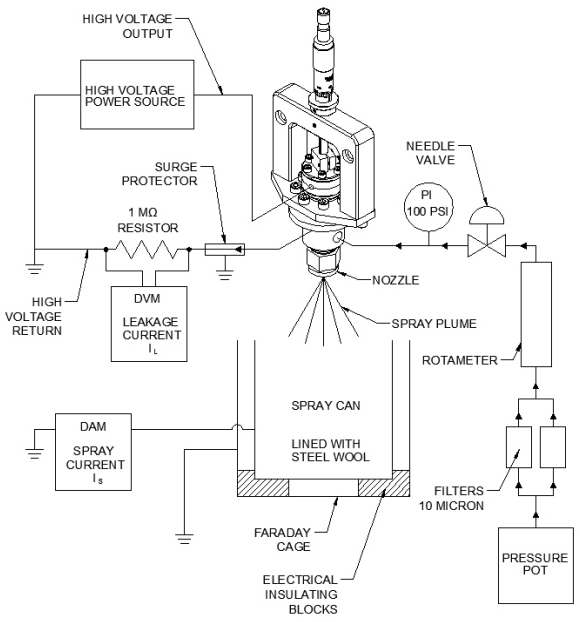

Figure 1. Schematic of Experiment Setup.

An Acopian N030HP1 high voltage power supply (HVPS) was used in this experiment to charge the nozzle. This HVPS generates a negative polarity voltage between 0 to -30 kV with the current limited to $0-1$ mA. Since this power supply contains analog meters for display of the output voltage and current, two Falcon F35 digital panel meters were wired to monitor these outputs providing a resolution of 100 V and 0.1 mA respectively.

The electrical performance of the nozzle was determined by measuring the leakage current, I_L; the current that leaks to the body of the nozzle, and the spray current, I_S; the current carried by the spray plume. The spray current was measured directly using a BK Precision 2831E digital multimeter (DMM) with a resolution of 0.1 μA. The spray current was generated by the collection of the charged spray on steel wool lining the spray can. With the small inter-electrode gaps used in this study, $0.06 \leq L \leq 0.30$ mm, there was risk of a catastrophic breakdown or arc between the two electrodes in the nozzle if dirt or air got in between them or if the voltage was too high. Attempting to measure the leakage current directly and without protection could lead to permanent damage to a DMM when a catastrophic breakdown occurs. To protect the DMM, a MTL-Instruments CA90F surge protector was used to safely discharge the current from the electrical discharge to ground. To further attempt to protect the DMM from damage in the event of an electrical

Figure 2. Electrostatic Atomizer.

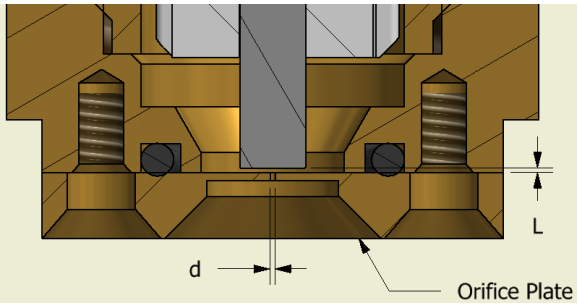

Figure 3. Section view of the electrostatic atomizer showing important the inter-electrode gap and orifice plate.

discharge, the voltage across a resistor was measured instead of directly measuring the current .

Drop size and velocity measurements were taken with an Artium 2D phase Doppler interferometry (PDI) system along with Artium Integrated Management Software (AIMS) version 4.4. This device measures size, velocity in two directions and arrival time for each particle that passes through the measurement volume generated by intersecting laser beam pairs. The PDI was setup with a 500 mm and 1000 mm focal length lenses for the transmitter and receiver respectively, providing a measurable drop size range of 2.6 to 385.6 μm. The receiver was positioned for the 40 degree off-axis forward scatter position as is shown in Fig. 4. The primary measurement channel utilized a pair of green, $\lambda = 532$ nm, lasers that measured droplet size and velocity in the positive z-direction, denoted by u_z. The second channel used a pair of red, $\lambda = 660$ nm, lasers and only measured droplet velocity in the positive x-direction, u_x. The phase Doppler measurement technique has been well studied and can be further reviewed in publications by Bachalo et al. [12]; also, the instrument setup and acquisition were performed in a manner similar to that described by Bade and Schick [13].

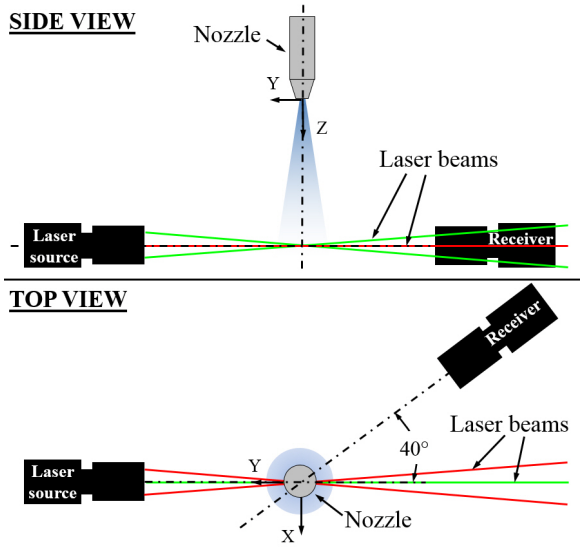

Figure 4. Artium 2D PDI Setup

The spray plume shape and distribution was analyzed using an Olympus i-SPEED TR high speed imaging (HSI) system and the LaVision, Inc. SprayMaster system. The HSI system can acquire videos with a frame rate up to 10,000 fps and with a maximum pixel resolution of 1280 x 1024 up to 2,000 fps. HSI was used to view the primary ligament breakup mechanism of the charge injection atomizer. The LaVision SprayMaster system was used to take laser sheet images (LSI) of planer cross sections of the spray. This system consisted of a LaVision Solo PIV Nd:YAG dual laser and high speed Imager Intense camera. The LSI system uses a short-duration pulsed laser that is passed through a divergent lens to illuminate the cross sections of the spray. This green $\lambda = 532$ nm laser sheet had a Gaussian intensity profile and is about 1 mm thick. A band-pass light filter is attached to the camera lens only allowing the light of the wavelength of the laser to pass to the CCD sensor. The liquid droplets scatter the laser light according to the Mie theory where the light intensity is equivalent to the surface area of the droplet. This system was used to qualitatively evaluate the spray plume shape and distribution. The SprayMaster system was calibrated before

use by first taking an image of a calibration sheet. This sheet contained rows and columns of uniformaly sized and spaced "+" symbols. The known size and spacing for these markings were entered into the DaVis 8.1 software to generate a correction transformation matrix. As is shown in Fig. 5, the camera is located at an off angle from the axis of the spray plume. This correction was performed by the software to transform the skewed, off-axis angle images to a view normal to the laser sheet. Sheet correction was also performed by acquiring a set of laser sheet images with the room filled with fog of nearly uniform droplet sizes. This allowed adjustment of the image intensities for the Gaussian intensity distribution of the laser sheet.

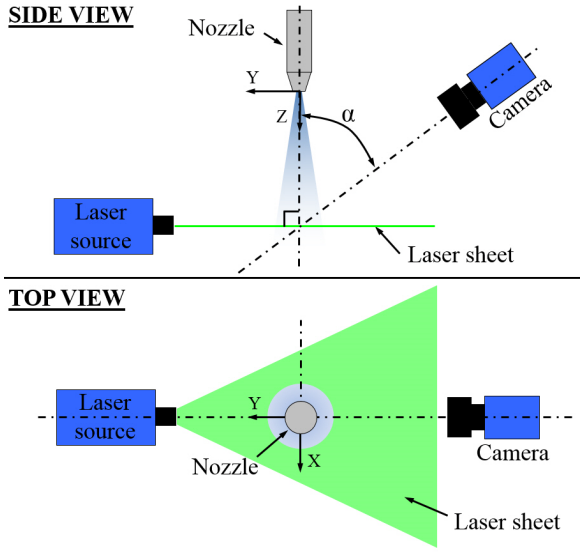

Figure 5. LaVision LSI Setup

Electrical Performance

The electrical performance of the electrostatic atomization nozzle was studied for various orifice diameters, L/d ratios and flow rates. The electrical performance was evaluated by calculating the total current, I_t, injected into the fluid as well as the volumetric spray specific charge, q_v, or just spray specific charge. These values are calculated by (1) and (2) below. The total current is the sum of both the leakage and spray currents whereas the spray specific charge is the ratio of the spray current to the volumetric flow rate of the oil.

$$I_t = I_s + I_l \tag{1}$$

$$q_v = \frac{I_s}{Q_v} \tag{2}$$

For the conditions tested, the electrical performance of the nozzle was evaluated by plotting total current and spray specific charge versus voltage as can be found in Figs. 10 through 17. Note the stepwise graph for spray specific charge. This is due to the resolution of the DMM used being of the same order of magnitude as the spray current values measured, which is not ideal. It appears that a linear relationship exists between both the total current and spray specific charge versus voltage. The spray specific charge reaches a maximum value before a sudden decrease to a value near, but above, zero. This is called the super-critical breakdown or partial breakdown condition where spray specific charge suddenly decreases but the total current continues to increase unaffected. For this condition, the charge injection is unaffected but the injected charge escapes to the nozzle body and by corona discharges in the air around the liquid jet before generating atomization. [14].

For both orifice diameters and jet velocities tested, the inter-electrode gap had the same impact on the total current and spray specific charge injected into the oil. Both of these values increased as the inter-electrode gap was increased. An increase in the jet velocity and its associated flow rate reduced the I_t and q_v for a given L/d and voltage. Table 2 shows the maximum spray specific charge for the various orifice diameters and flow rates tested. The maximum spray specific charge increased for higher flow rates but was reduced when the orifice diameter was increased from $150\mu m$ to $200\mu m$. The observations discussed for the total current and spray specific charge versus voltage follows expected trends displayed in previous studies by Rigit et al. [7], Malkawi [15] and others. Note, for Table 2, the length scale used to calculate Re and We numbers was the orifice diameter.

d (μm)	Q_v $\left(\frac{ml}{min}\right)$	u_j $\left(\frac{m}{s}\right)$	$q_{v,max}$ $\left(\frac{C}{m^3}\right)$	Re	We
150	10.6	10	3.9	20.7	382
	15.9	15	4.1	31.0	859
200	18.8	10	2.2	27.5	509
	28.3	15	2.5	41.3	1145

Table 2. Maximum spray specific charge achieved for Soybean Oil with $L/d = 0.8$.

Spray Plume Charactization with HSI and LSI

The characteristics of the spray plume were investigated using HSI and LSI. Fig. 6 shows the primary breakup mechanism for the charge injection electrostatic atomizer. Perturbations develop in the solid jet that exits the nozzle, which moves the charges on the surface of the jet closer to each other. The mutual repulsion of the like charges bend the solid jet forming the expanding helical pattern shown in Fig. 6. Eventually, the helical ligaments stretch too far and break apart into droplets [16]. The secondary atomization is not visible in Fig. 6, but can be seen in Fig. 7. Small droplets with high charge to mass ratio escape from the larger droplets in the spray plume. These smaller droplets are fairly uniform in size and initially move normal to the direction of the larger drops they escape from. They move slowly with respect to the larger droplets in the spray plume, and are easily carried by the electrical field generated by the nozzle along with air currents. The majority of these drops collect on the nozzle body or on neighboring surfaces, which makes it important to ground all surfaces in the vicinity of the electrostatic atomizer to prevent the buildup of charge and the chance for static discharge. From this testing with soybean oil, the small droplets could not be eliminated but could be greatly reduced by lowering the voltage. When the nozzle is operating near maximum spray specific charge, it is generating a significant amount of these small, highly charged droplets.

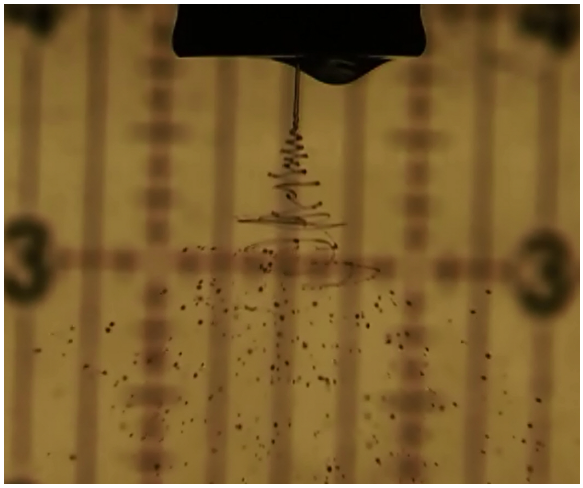

Figure 6. HSI for $d = 150\mu m$, $L/d = 0.8$, $u_j = 10m/s$ and $q_v = 2.2C/m^3$ recorded at 5,000 fps.

Fig. 8 shows laser sheet images taken at various distances from the nozzle. 1500 images were taken at each height from the nozzle, were averaged into a single image and then corrected for the camera angle. The electrostatic atomizer makes a full cone spray pattern. At a distance of 40 mm from the nozzle, the spray plume was very concentrated as is shown by the dark red in the center of the spray as is shown in Fig. 9. Note, the green trail above the spray plume in this figure (in the +y region around x=0) is due to the illumination of the spray plume above the laser sheet due to the scattering of the laser sheet light. At further distances from the nozzle, the spray plume expands and becomes less dense. The small droplets generated by secondary atomization are not easily captured by the LSI system, but the very faint outer-spray is primarily made up of these droplets. These small droplets have very small surface area, hence, did not scatter as intense of a light on the camera as the larger droplets did.

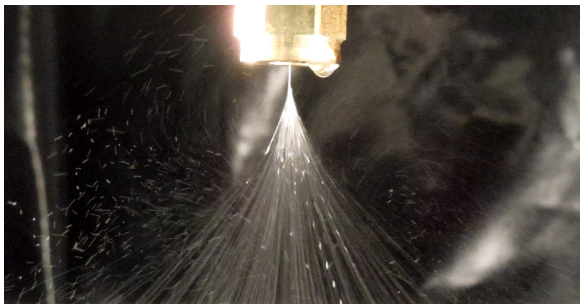

Figure 7. Electrostatic atomizer operating with $d = 200\mu m$, $L/d = 1.0$, $u_j = 10m/s$ and $q_v = 2.2C/m^3$.

Drop Size and Velocity Measurements with the PDI

The drop size statistics and velocities were measured using a PDI system and the results are shown in Figs. 18 through 25. The arithmetic mean diameter, D_{10}, mean volume diameter, D_{30}, and the Sauter mean diameter, D_{32} are plotted versus radial position from the center of the spray for the conditions tested. The drops size, D, spray distance, z, and the radial position, r, were all normalized by the orifice diameter, d. Drop size measurements were taken for the operating conditions of 150 and 200 μm orifice diameters, 10 and 15 m/s jet velocities and an L/d ratio of 0.8 with the nozzle operating steadily under maximum spray specific charge.

For the drop size statistics for both orifice diameters and flow rates tested, the curves followed expected trends from what was observed from the

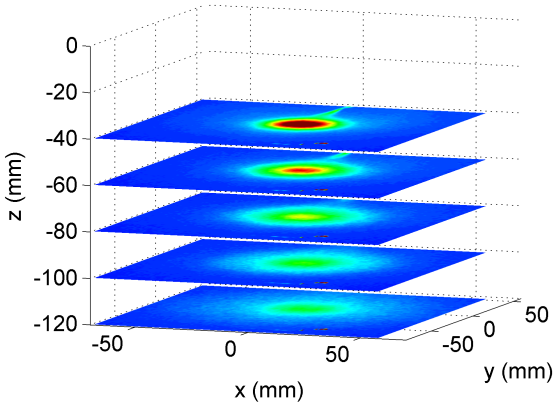

Figure 8. LSI for $d = 200\mu m$, $L/d = 0.8$, $u_j = 10m/s$ and $q_v = 1.2C/m^3$ at various distances from the nozzle.

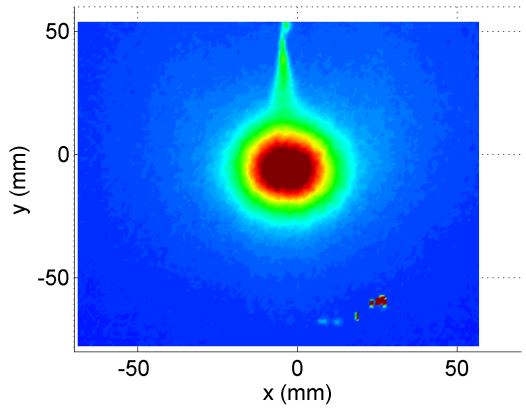

Figure 9. LSI at 40 mm from the nozzle.

HSI and standard image from Figs. 6 and 7. The larger droplets made up the main spray plume while outside the main spray plume resided much smaller and slowly moving droplets. In Fig. 18, the D_{32} is the same as the orifice diameter. When the jet velocity is increased as is shown in Fig. 19, smaller droplets were produced. The higher pressure needed to generate the higher jet velocity of this high viscosity oil through such a small orifice diameter added to the energy of the spray and contributed to the generation of the smaller droplets. When the orifice diameter is increased to 200 μm, nearly the same D_{32} of about 150 μm is measured in the spray plume for the $u_j = 10m/s$ case. The required pressure to generate this jet velocity is low, the electrical energy injected into the oil is the primary driver of atomization. For all orifice diameters and jet velocities tested, the largest droplets were towards the edge of the spray plume with slightly smaller droplets filling in the center. Very small droplets drifted from the spray plume to the far-outer regions. For all cases tested, these very small droplets ranged from about $30 \leq D \leq 40$ μm. The droplets from secondary atomization are not ideal but the quantity of them can be reduced by lowering the voltage, hence spray specific charge, and are easily captured on grounded, conductive plates or meshing.

Similar drop size trends have been previously published by Shrimpton et al. [6] for kerosene, which has a dynamic viscosity around 1.3 cP. This is roughly 2% that of soybean oil. Both soybean oil and kerosene have similar surface tension, which are 33 dyn/cm and 25 dyn/cm respectively. This seeming independence in viscosity would be an important advantage of spraying these types of dielectric fluids via electrostatic atomization nozzle instead of a traditional hydraulic nozzle of which spray performance is greatly affected by the viscosity of the fluid. Further work on this investigation needs to be done to justify a viscosity independence nature of spraying a dielectric fluid with an electrostatic atomization nozzle.

The velocity vector fields generated from the 2D PDI show that the larger droplets within the main spray plume have the largest velocity while the small droplets that escaped the main plume move very slowly. These smaller droplets generally move away from the spray plume and are carried in air currents and by the electric field generated by the primary spray plume and nozzle.

Conclusion

This study investigates the viability in spraying soybean oil for coating applications via an electrostatic atomizing nozzle. Various orifice diameters and jet velocities were studied for their effect on drop size. It was shown that the nozzle produced a full cone spray plume with fairly uniform spray coverage at 100 mm and further from the nozzle. Secondary atomization does generate undesired small droplets that drift with air currents but are charged and easily captured on grounded conducting plates or mesh. The low nozzle pressure and resulting jet velocity are ideal for oil coating applications as the charged, larger droplets low momentum and easily collect and stick onto the intended target to be coated. The potential of the electrostatic atomizer's performance being independent of viscosity would be a great benefit for using this nozzle over conventional hydraulic nozzles for oil coating processes and warrants further investigation.

Nomenclature

D	drop diameter
d	orifice diameter
I	current
L	inter-electrode gap
n	refractive index
Q	flow rate
q	charge
r	radial position
u	velocity
V	voltage
λ	wavelength
μ	dynamic viscosity
ρ	density or resistivity
σ	surface tension

Subscripts

e	electrical
l	leakage
j	jet
max	maximum
s	spray
t	total
v	volumetric
x	x-direction
z	z-direction

References

[1] C. D. Cooper and F. C. Alley. *Air Pollution Control, A Design Approach*. Waveland Press, Inc, Long Grove, IL, 4th edition, 2011.

[2] W Kalata, K Brown, S O Donnell, and R J Schick. *ILASS Americas 26th Annual Conference on Liquid Atomization and Spray Systems*, Portland, OR, May 2014.

[3] Kyekyoon Kim and Robert J. Turnbull. *Journal of Applied Physics*, 47(5):1964–1969, 1976.

[4] Kelly S. Robinson, Robert J. Turnbull, and Kyekyoon Kim. *IEEE Transactions on Industry Applications*, IA-16(2), 1980.

[5] A.J. Yule, J.S. Shrimpton, A.P. Watkins, W. Balachandran, and D. Hu. *Fuel*, 74(7):1094–1103, 1995.

[6] J.S. Shrimpton and A. J. Yule. *Experiments in Fluids*, 26:460–469, 1999.

[7] A.R.H. Rigit and J.S. Shrimpton. *Atomization and Sprays*, 16:401–419, 2006.

[8] E L Ergene, A Kourmatzis, J Komperda, R J Schick, J S Shrimpton, and F Mashayek. *ILASS Americas, 23rd Annual Conference on Liquid Atomization and Spray Systems*, Ventura, CA, May 2011.

[9] Earl G Hammond, Lawrence a Johnson, Caiping Su, Tong Wang, and Pamela J White. Soybean Oil. In Fereidoon Shahidi, editor, *Bailey's Industrial Oil and Fat Products*, pp. 577–653. John Wiley & Sons, Inc., 6th edition, 2005.

[10] A.R.H. Rigit and J.S. Shrimpton. *Atomization and Sprays*, 16:421–442, 2006.

[11] A. Alj, A. Denat, J.P. Gosse, B. Gosse, and I. Nakamura. *Electrical Insulation, IEEE Transactions on*, EI-20(2):221–231, April 1985.

[12] W.D. Bachalo and M.J. Houser. *Optical Engineering*, 23(5):583–590, 1984.

[13] Kyle M. Bade and R. J. Schick. *Atomization and Sprays*, 21(7):537–551, 2011.

[14] John Shrimpton and Farzad Mashayek. *47th AIAA Aerospace Sciences Meeting Including The New Horizons Forum and Aerospace Exposition*, pp. 1–36, Orlando, FL, January 2009.

[15] Ghazi Malkawi. Phd thesis, University of Illinois at Chicago, 2009.

[16] G. Malkawi, a. L. Yarin, and F. Mashayek. *Journal of Applied Physics*, 108(6), 2010.

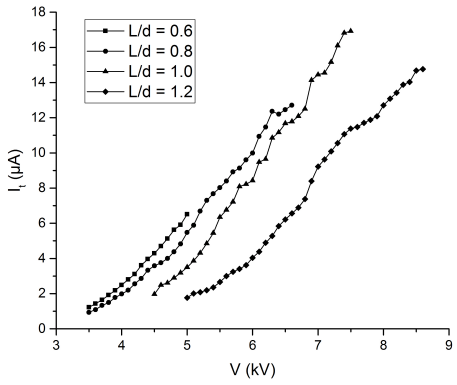

Figure 10. Total current vs voltage for $d = 150\mu m$ and $u_j = 10m/s$

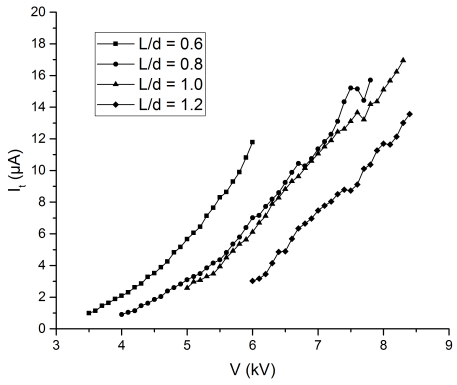

Figure 12. Total current vs voltage for $d = 150\mu m$ and $u_j = 15m/s$

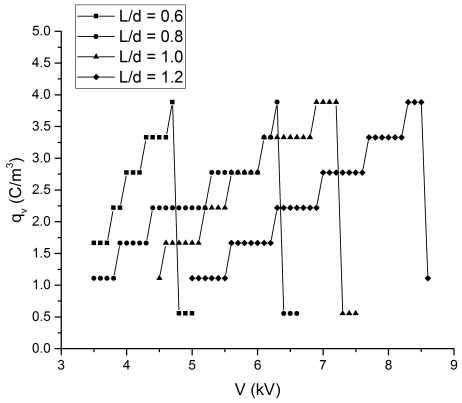

Figure 11. Spray specific charge vs voltage for $d = 150\mu m$ and $u_j = 10m/s$

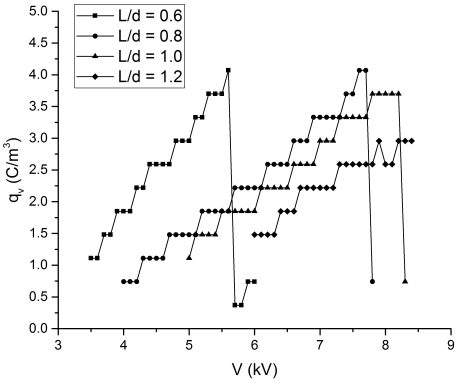

Figure 13. Spray specific charge vs voltage for $d = 150\mu m$ and $u_j = 15m/s$

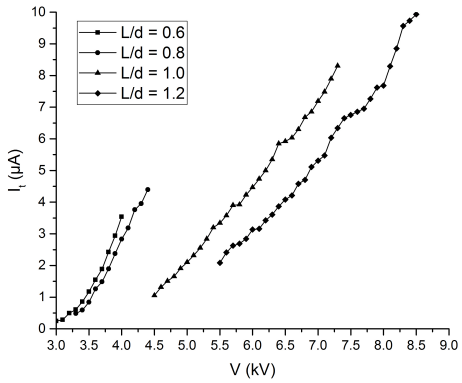

Figure 14. Total current vs voltage for $d = 200\mu m$ and $u_j = 10m/s$

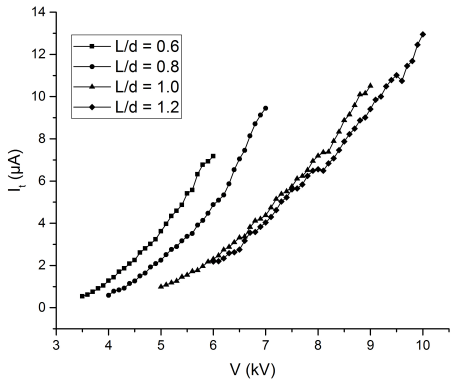

Figure 16. Total current vs voltage for $d = 200\mu m$ and $u_j = 15m/s$

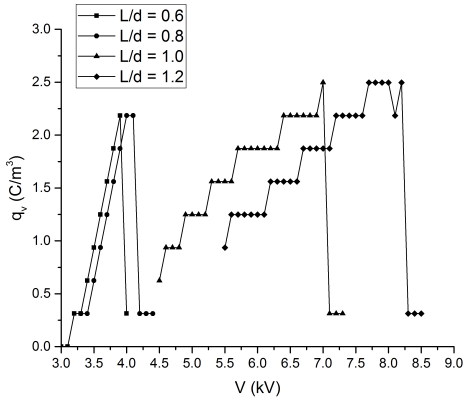

Figure 15. Spray specific charge vs voltage for $d = 200\mu m$ and $u_j = 10m/s$

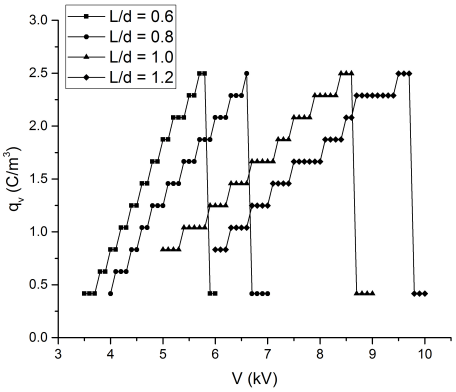

Figure 17. Spray specific charge vs voltage for $d = 200\mu m$ and $u_j = 15m/s$

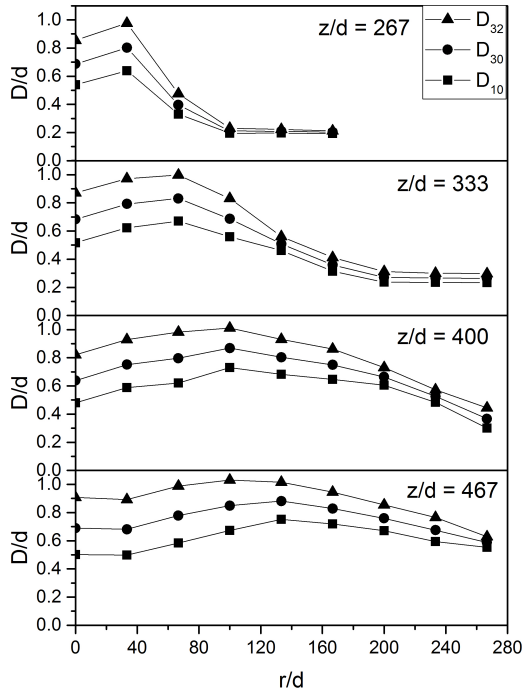

Figure 18. Normalized point drop size statistics for $d = 150\mu m$, $L/d = 0.8$, $u_j = 10m/s$ and $q_v = 2.8C/m^3$.

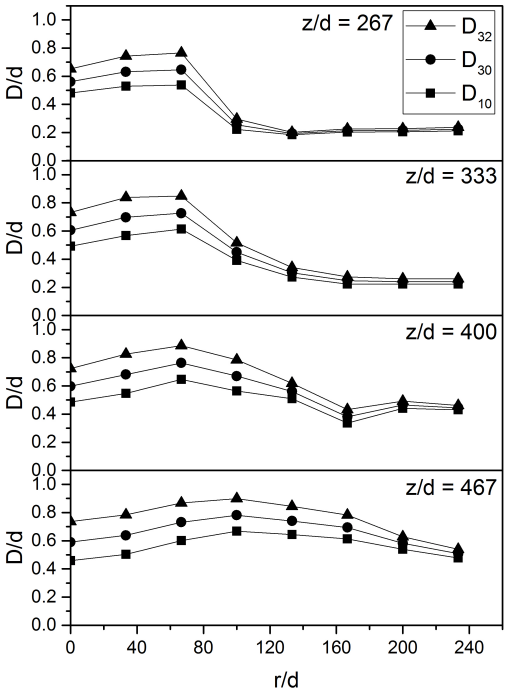

Figure 20. Normalized point drop size statistics for $d = 150\mu m$, $L/d = 0.8$, $u_j = 15m/s$ and $q_v = 2.8C/m^3$.

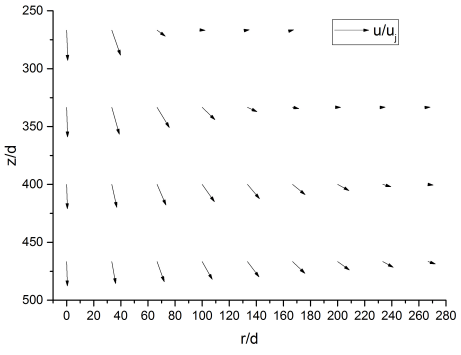

Figure 19. Velocity vector field for $d = 150\mu m$,$L/d = 0.8$, $u_j = 10m/s$ and $q_v = 2.8C/m^3$.

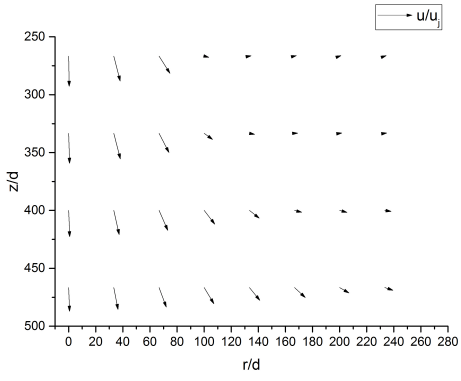

Figure 21. Velocity vector field for $d = 150\mu m$, $L/d = 0.8$, $u_j = 15m/s$ and $q_v = 2.6C/m^3$.

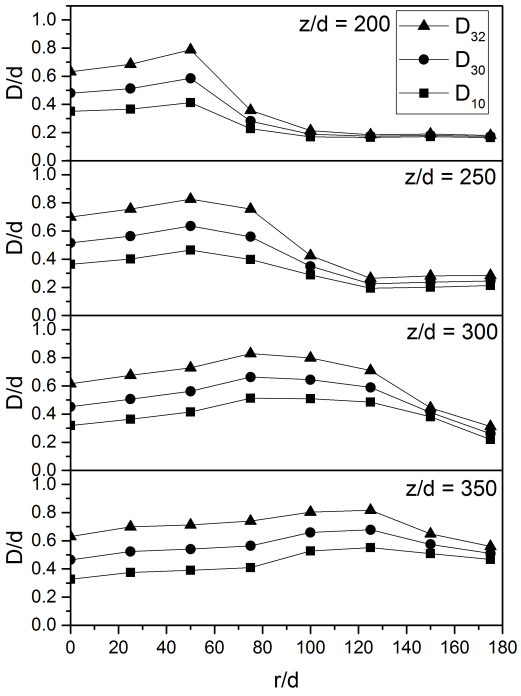

Figure 22. Normalized point drop size statistics for $d = 200\mu m$, $L/d = 0.8$, $u_j = 10m/s$ and $q_v = 2.2C/m^3$.

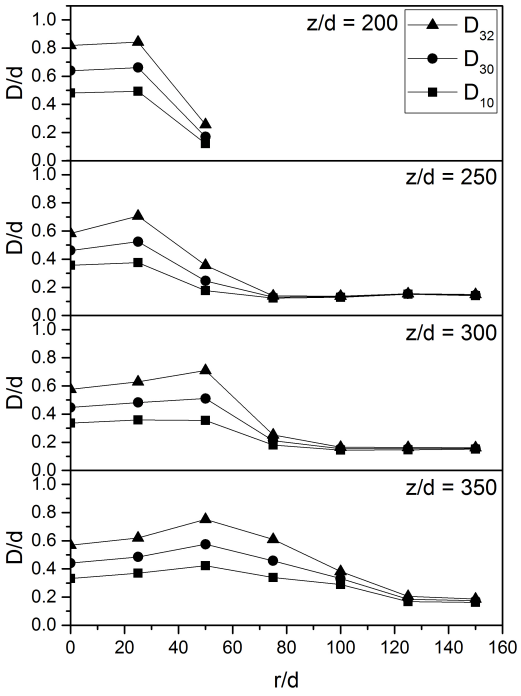

Figure 24. Normalized point drop size statistics for $d = 200\mu m$, $L/d = 0.8$, $u_j = 15m/s$ and $q_v = 2.3C/m^3$.

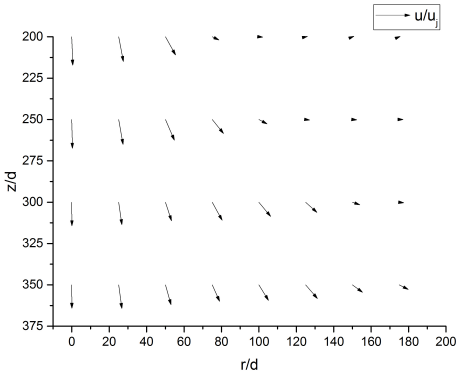

Figure 23. Velocity vector field for $d = 200\mu m$, $L/d = 0.8$, $u_j = 10m/s$ and $q_v = 2.2C/m^3$.

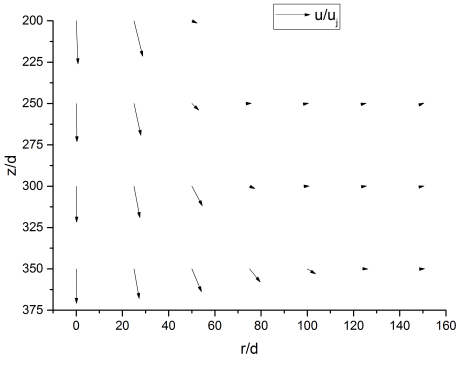

Figure 25. Velocity vector field for $d = 200\mu m$, $L/d = 0.8$, $u_j = 15m/s$ and $q_v = 2.3C/m^3$.